

# Design and Measurement of the Sextupole Magnet for the APS Storage Ring\*

L. R. Turner, K. M. Thompson, S. H. Kim, K. Kim  
Advanced Photon Source, Argonne National Laboratory  
9700 S. Cass Avenue, Argonne, Illinois 60439

## Abstract

A prototype sextupole magnet has been designed, constructed, and measured for the storage ring of the Advanced Photon Source. The design approaches very closely to  $120^\circ$  rotation symmetry, in order to minimize all forbidden multipole components. The core is made of three identical stacks of laminations, each lamination consisting of two poles and the return yoke joining them. The antechamber of the thick aluminum vacuum chamber fits between two neighboring stacks. Computations and measurements of the sextupole strength  $B''$  and multipole field components, both in the central region and integrated in the beam direction, show that the magnet meets the requirements for positron beam dynamics.

## 1. INTRODUCTION

The storage ring of the Advanced Photon Source (APS) produces synchrotron radiation for experiments in material science, biomedical research, and other fields. The ring maintains a 7-GeV positron beam for a lifetime of 10 hours or more. The ring includes 280 sextupole magnets to control the chromaticity of the positron beam. These sextupole magnets operate at a strength of up to  $405 \text{ T/m}^2$  and have an effective length of 0.24 m.

The long beam lifetime requires a vacuum of 1 nTorr or better, but synchrotron radiation desorbs gases from the vacuum chamber, leading the vacuum to degrade. For this reason, the vacuum chamber of the APS consists of two chambers; the antechamber entraps the outgassing and high-speed distributed pumping removes it.

This large, two-chambered vacuum chamber makes the design of the magnets for the storage ring more difficult. Earlier designs for the ring sextupole did not exhibit the  $120^\circ$  symmetry of an ideal sextupole, and both computation and measurement showed the presence of unacceptable dipole and other forbidden multipole components of the field.

## II. DESIGN OF THE SEXTUPOLE

Figure 1 shows a photograph of the ring sextupole magnet, and the cross section is seen in Fig. 2. The design approaches very closely to  $120^\circ$  rotation symmetry, in order to minimize all forbidden multipole components. Table 1 lists some of the parameters.

\*Work supported by the U.S. Department of Energy, Office of Basic Energy Sciences, under Contract No. W-31-109-ENG-38.

The magnet is excited with six coils made of water-cooled copper conductor insulated with a preapplied polyimide/polyester/glass film and vacuum-impregnated epoxy. The coils extend beyond the ends of the core; no steel need be removed from the core corners under the coils.

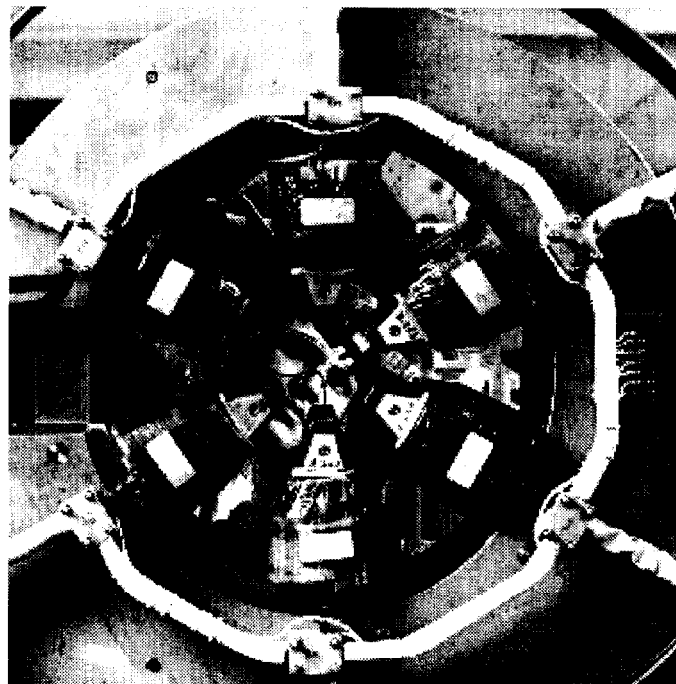


Figure 1. Prototype sextupole magnet for the APS storage ring.

Table 1  
Parameters for the Storage Ring Sextupole  
(7.0 GeV Operation)

Effective Length	0.24 m
Central Field Strength	$405 \text{ T/m}^2$
Bore Diameter	98 mm
Magnetic Core Length	0.21 m
Maximum Current	161 A
Number of Turns per Pole	42
Maximum Power Losses	2.8 kW
Coolant Temperature Rise	$8.6 \text{ }^\circ\text{C}$

The magnet core is assembled from three identical stacks of laminations, each with two poles and the return path joining them. The antechamber of the thick aluminum vacuum chamber lies in one of the 102-mm air gaps between neighboring stacks. The 1.52-mm-thick laminations are made of low-carbon steel, coated on both sides with a 13- $\mu\text{m}$ -thick B-stage epoxy. During curing in a precision fixture, tie bars and tie rods are also epoxy bonded into the core. At each end 12.7-mm-

thick stainless steel plates hold the core sections in position; they are pinned and bolted to the core sections with an assembly fixture.

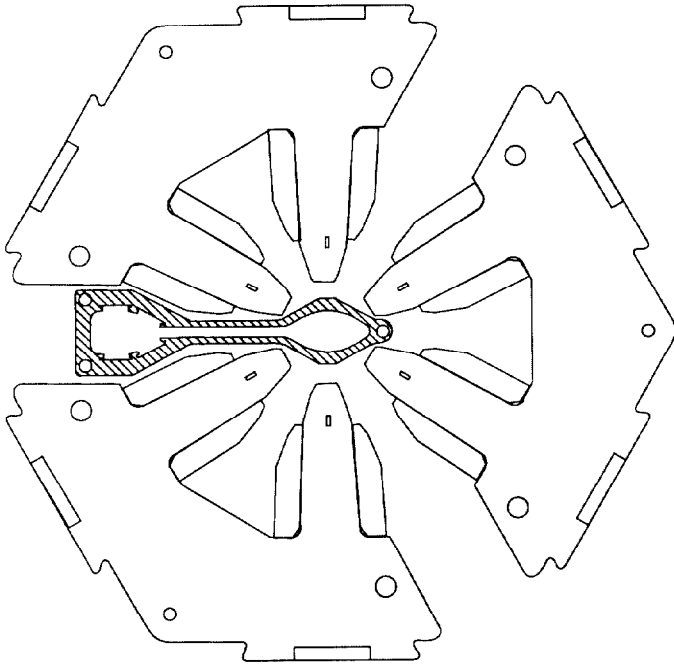


Figure 2. Cross section of the storage ring sextupole magnet with vacuum chamber.

### III. COMPUTATION OF THE SEXTUPOLE

Computations were carried out with the 2-D finite-element code PE2D and the 3-D code TOSCA [1]. As the effective length of the magnet is 0.24 m while the core length is 0.21 m, the flux density is higher in the magnet poles than it would be for a longer magnet with the same ampere-turns. Thus measurement and 3-D computation show the onset of saturation effects where 2-D computation does not.

With this design, in the absence of assembly misalignments there can be no forbidden multipole terms; any that appear in the computation must be artifacts of the mesh and/or of the field evaluation within the mesh. The first allowed multipole beyond the sextupole is the 18-pole. The pole tips were deliberately made narrower than optimum for this magnet to facilitate installing the coils over the poles. A consequence is a negative 18-pole component of about 0.12% at a reference radius of 25 mm. Beam orbit computations show that an 18-pole field of this size has no influence on the dynamic aperture [2]. The multipole field ratios were found by computing the potential over an arc of a circle, and then fitting the potential to a multipole series using the HARM subroutine from the code POISSON [3]. Measured and computed multipoles are compared below in Table 2.

In the bore region, the sextupole field varies quadratically with position. Hence the analysis should be carried out with third-order finite elements, which exhibit quadratic field variation. PE2D, TOSCA, and most other codes support only first- and second-order elements. This limitation can be overcome

in part by using a finer mesh with more elements, but at the cost of more computing time and memory. Even with the finer mesh, computing magnet parameters must be done with care since the computed field varies only linearly within each element.

In the 2-D computations, three kinds of triangular meshes were generated over the bore region and compared: (a) an adaptive mesh automatically generated in the polygonal regions of the bore; (b) a regular annular mesh, defined between radii 5 mm and 42 mm and over 30° of arc, then reflected to fill the 180° or 360° considered; and (c) an equilateral triangular mesh generated over a 60° parallelogram then reflected to form a hexagon. In all three cases, an adaptive mesh was used outside the regions specified. It was predicted [4] that an equilateral mesh gives a potential (at the nodes) correct to sixth order. How the potential varies within a triangular element depends upon the interpolation methods supported by the code. For the 3-D computations, a hexahedral mesh was used, square in the plane perpendicular to the beam direction. This mesh should result in a potential (at the nodes) correct to fourth order [4].

In the bore of a sextupole magnet, the ratio  $B/r^2$  should be constant, where  $B$  is the modulus of flux density and  $r$  is radial distance from the beam centerline. Contour plots of this ratio showed it to vary less for the annular mesh than for the adaptive, and less for the equilateral than for the annular.

### IV. MEASUREMENT OF THE SEXTUPOLES

The sextupole strength and the multipole coefficients (ratio of a specified multipole field to the sextupole field) were measured for the prototype ring sextupole SSX-2. In each case both the integrated (3-D) and body (2-D) fields were measured, using a rotating-coil technique [5]. The probe consisted of an 0.8-m-long radial coil for the 3-D measurements and an 0.08-m-long tangential coil for the 2-D measurements. The radial coil extended well beyond the magnet and the fringe field regions at either end. The tangential coil was located entirely within the magnet, away from the end regions. Measurements were taken at a radius of 35.7 mm, and the multipole coefficients were normalized to a 25-mm radius. Before measurements were made, the magnetic axis of the sextupole was aligned to the axis of the rotating coil.

In Fig. 3, the ratio of integrated sextupole field strength to excitation current is plotted against current. At low currents the ratio is independent of current; the excitation efficiency is said to be 100%. Above 150 A, effects of steel nonlinearity begin to enter, and the excitation efficiency decreases steadily. In Fig. 4 the same ratio is plotted for the body (2-D) sextupole field strength. The 3-D efficiency is seen to be only 0.6% lower than the 2-D efficiency.

Field multipole coefficients were determined from the measurements. Table 2 shows the 18-pole coefficient  $b_8$  is large and negative, it is found to be largely independent of current. The 10-pole component  $b_4$  (both body and integrated) was observed to increase from  $1 \times 10^{-4}$  to  $3 \times 10^{-4}$  as the current increased from 50 to 200 A. All other field multipoles were about  $1 \times 10^{-4}$  or smaller over the total current range.

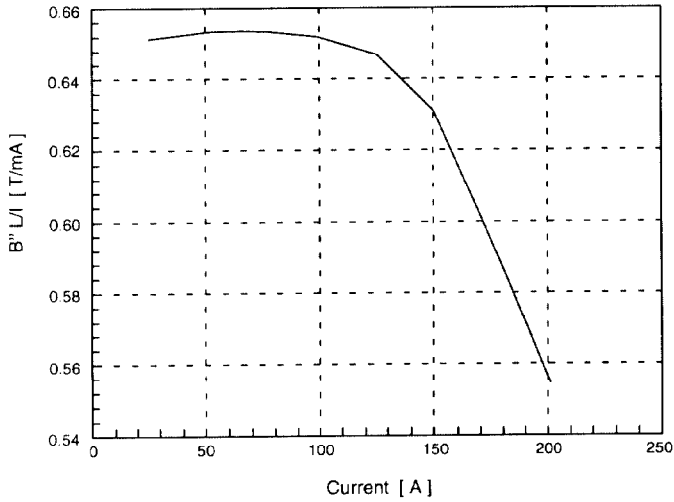


Figure 3. Variation of the ratio of integrated sextupole strength to current ( $B''L/I$ ) with current I.

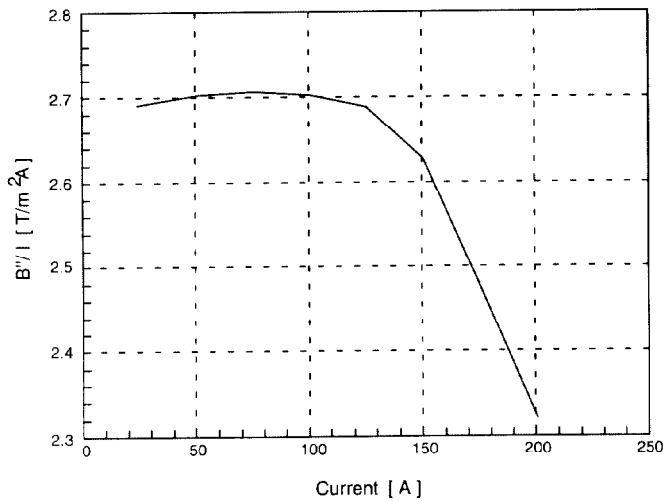


Figure 4. Variation of the ratio of body sextupole strength to current ( $B''/I$ ) with current I.

Table 2  
Ratio of 18-Pole to Sextupole Field at 200 A  
( $\times 10^{-4}$  at the reference radius of 25 mm)

	Computed	Measured
2-D (Body)	-12.2	-11.5
3-D (Integrated)	-13.1	-12.7

## V. CONCLUSIONS

Geometrical and field measurements of the prototype demonstrated that the design and the assembly method will produce magnets that meet the requirements of the positron beam dynamics and production schedule. To reduce the saturation effects demonstrated in the magnetic field measurements, the core length of production magnets will be increased by 6% (12.7 mm). The overall length of the magnets will not be changed.

## VI. REFERENCES

- [1] Codes PE2D (now called OPERA-2D) and TOSCA are available from Vector Fields, Inc., Aurora, IL, USA.
- [2] Eliane Lessner, Argonne National laboratory, personal communication.
- [3] POISSON is available from the Los Alamos Accelerator Code Group, Los Alamos National Laboratory.
- [4] Klaus Halbach, Lawrence Berkeley Laboratory, personal communication.
- [5] S. H. Kim, K. Kim, C. Doose, R. Hogrefe, and R. Merl, "Magnet Measurement Facility for the 7-GeV Advanced Photon Source," these proceedings.